Punjab University
Journal of Mathematics (ISSN 1016-2526)
Vol. 43 (2011) pp. 47-67

Analysis of Stresses and Power Consumption of Mixing Flow in Cylindrical Container

R. A. Memon
Centre for Advance Studies in Pure and Applied Mathematics,
Bahauddin Zakria University,
Multan, Punjab, Pakistan.
Email: ra-memon1@yahoo.com

M. A. Solangi
Department of Basic Sciences and Related Studies,
Mehran University of Engineering and Technology,
Jamshoro, Sindh, Pakistan.
Email: manwarsolangi@yahoo.com

A. Baloch
Department of Basic Sciences and Related Studies,
Mehran University of Engineering and Technology,
Jamshoro, Sindh, Pakistan.
Email: csbaloch@yahoo.com

Abstract: This research article addresses the mixing flow of Newtonian fluid in a cylindrical vessel and investigates the rotational speeds and rotational directions of double stirrer cases on the predictions of the power consumption in the dissolution rotating vessel configured with fixed and rotating stirrers. The numerical simulations are sought for incompressible rotating mixing flows of Newtonian fluid. The context is one, relevant to the food industry, of mixing fluid within a cylindrical vessel, where stirrers are located on the lid of the vessel eccentrically. Here, the motion is considered as driven by the rotation of the outer vessel wall, with various rotational speeds of vessel and stirrers. A time-stepping finite element method is employed to predict the solutions. The numerical technique adopted is based on a semi-implicit TGPC scheme, posed in a two-dimensional cylindrical polar coordinate system. In mixer geometry, with respect to the velocity gradient, shear-rate, shear stress and power consumption are analysed.

AMS (MOS) Subject Classification Codes: 65N30, 65M60, 74S05, 68Q05, 76D05, 35Q30, 76U05
Key Words: Numerical Simulation, Finite Element Method, Rotational Mixing Flows, Newtonian Fluids, Double Stirrers, Co-rotation, Contra-rotation, Mix-rotation, Power Consumption.

1. Introduction

Mixing flows within the cylindrical vessel are investigated in this article, and is the extension of the previous work to achieve the solution of industrial challenging problems in mixing processing, the design of the mixer with rotational mixing in a stirred vessel to predict power consumption, generally industrial problems are challenging to deal with, particularly in the field of chemical process applications, such as mixing of dough in a food processing industry [1, 2, 3, 4, 5], granular mixing, powder mixing processes [6], mixing of paper pulp in paper industry and many other industrial processes. The present problem is one of these forms, expressed as the flow between an outer rotating cylindrical vessel and double stationary and rotating cylindrical stirrers rotate in three different rotational directions (co-rotating, contra-rotating and mix-rotating directions) and three different speeds (half, same and double) of the stirrers against the speed of the cylindrical vessel.

Stirrers are located on the mixing vessel lid. Under two-dimensional assumptions, the vessel essentially is considered to have infinite height. Elsewhere, the finite vessel problem in three-dimensions [6, 7] has been analysed. In two-dimension, similar problem is also investigated with different number and shapes of stirrers [8, 9, 10]. The motivation for this work is to advance fundamental technology in modelling of the dough kneading with the ultimate aim to predict the optimal design of dough mixers themselves, hence, leading to efficient dough processing.

The simulation procedure addresses the numerical solution of the two-dimension Navier-Stokes equations for incompressible flow in cylindrical frame of reference. This involves a so-called Taylor-Galerkin finite element formulation, which applies a temporal discretisation in a Taylor series prior to a Galerkin spatial discretisation. A semi-implicit treatment for diffusion is employed to address linear stability constraints. The flow is modelled as incompressible via a pressure-correction scheme [8, 9, 10, 11]. The present study adopts a semi-implicit Taylor-Galerkin/Pressure-Correction (TGPC) time-marching scheme, which has been developed and refined over the last couple of decades. This scheme, initially conceived in sequential form, is appropriate for the simulation of incompressible Newtonian flows [11].

The object is to comprehensively examine the influence of speed of stirrers and variation in inertia, assessing how this imposes upon the flow structure, rate-of-work done generated and power consumption. The corresponding applications of dough kneading are the target through build-up of the material structure, achieved by maximizing the local rate-of-work done per unit power. Computations are performed for Newtonian fluid.

In Section 2, the complete problem is specified and the governing equations and numerical scheme are described in Section 3. This is followed, in Section 4, by Simulation results for all cases are presented and our conclusions are drawn in Section 5.

2. Problem specification

The two-dimensional mixing flows of Newtonian fluids are investigated, relevance to the food industry. In reality, within the industrial process, fluid is driven by the rotation of the lid of the vessel would rotate with stirrers attached. For simulations, the mixing is performed through the rotation of cylindrical-shaped vessel and the stirrers are held in place by being attached to the lid of the vessel. A fixed and rotating double stirrer in an eccentric configuration is adopted. Initially, the problem is analysed for rotating flow between stationary stirrers and rotating cylindrical vessel, to validate the finite element predications in this cylindrical polar co−ordinate system to compare the numerical results against results obtained in previous investigations [8, 9]. Subsequently, different rotational directions with three setting options (co−rotation, contra−rotation and mix−rotation) of stirrers are also investigated against stationary stirrers in a rotating cylindrical vessel.

In this study, solution fields of interest are presented through contour plots of velocity gradients (∇u), shear−rate ($\dot{\gamma}$), shear−stress($\tau_{r\theta}$), hoop and radial stress difference ($N_1 = \tau_{\theta\theta} - \tau_{rr}$) and power ($\dot{P}$). Power may be equated to the spatial integral of the rate-of-work done where I_2 is the second invariant of rate-of-deformation tensor and w is rate of work done over total time t_n, v_r and v_θ are velocity components in radial 'r' and azimuthal 'θ' direction respectively and ω is domain of interest in two dimensional polar coordinate.

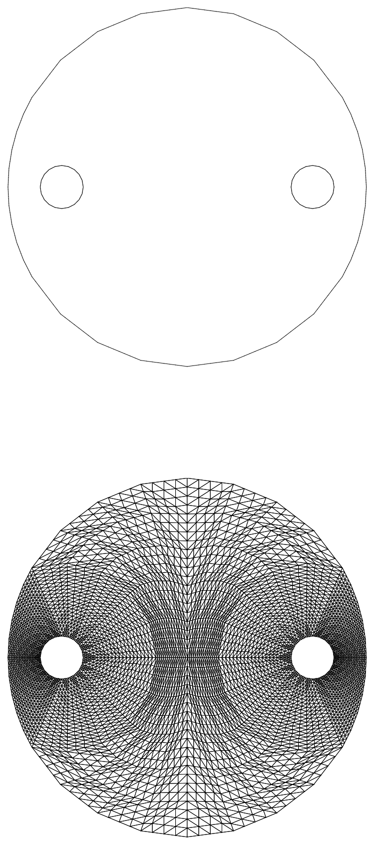

FIGURE 1. Computational domain and finite element mesh of eccentric rotating cylinderical flow, with double stationary and rotating stirrers.

Domain and finite element mesh for the problem involved is shown in figure−1. Total number of elements, nodes and degrees−of−freedom are 8960, 18223 and 40057 respectively. Details on mesh convergence, initial and boundary conditions reader is referred to our pervious investigations [7, 8, 9]. In this study, solution fields of interest are presented through contour plots of velocity gradients, shear−rate, shear−stress and power. Power may be equated to the spatial integral of the rate−of−work done [8, 9].

3. Governing System of Equations and Numerical Scheme

Two-dimensional incompressible rotational flows of isothermal Newtonian fluids can be modelled through the continuity and generalised momentum transport equations in a cylindrical polar coordinate system. In the absence of body forces, after applying appropriate scaling in each variable (u=Vu*, p = V^2 p*, t = R t*/ V, where R and V are characteristic radius and velocity of vessel respectively and the time divided by the characteristic time) takes the form of the non-dimensional system of equations can be represented through the conservation of mass equation, as,

$$\nabla \cdot \mathbf{u} = 0, \tag{3. 1}$$

the conservation of momentum transport equation, as,

$$\frac{\partial \mathbf{u}}{\partial t} = \frac{1}{Re}\nabla^2\mathbf{u} - \mathbf{u}\cdot\nabla\mathbf{u} - \nabla p, \tag{3. 2}$$

where, **u** is the fluid velocity vector field, p is the isotropic fluid pressure (per unit density), **d** is the rate of deformation tensor, t represents time and ∇ is the spatial differential operator. For Newtonian fluid case, μ_0 is the corresponding constant fluid viscosity at zero shear-rate. Relevant non-dimensional Reynolds number is

$$Re = \frac{\rho V R}{\mu_0} \tag{3. 3}$$

.

The characteristic velocity V is taken to be the rotational speed of the vessel, the characteristic length scale is the radius, R, of a stirrer and is the fluid density. A detail on numerical algorithm, fully discrete system and definition of matrices is described and can be found in [8, 9, 11, 12].

4. Numerical Results and Discussions

The predicted solutions are analysed in two different directions: change in rotational direction (co−rotating, contra−rotating and mix−rotating) and speed of the stirrers. This leads to testing with respect to increasing viscosity levels for Newtonian fluid, comparison of contour plots of velocity gradient, shear-rate, shearstress and power consumption across problem instances. Contours are plotted from minimum value to maximum value, over a range. Numerical solutions are also analysed through graph of work done over time interval and power consumption. Comparative diagnostics may be derived accordingly.

Various increasing levels of zero-shear viscosities μ_0 are considered, from which Reynolds numbers are computed, as defined above. For Reynolds numbers Re = 8.0, Re = 0.8 and Re = 0.08, the corresponding zero shear viscosities are μ_0 = 1.05 Pa s, μ_0 = 10.5 Pa s and μ_0 = 105.0 Pa s. respectively. Of these levels, a range of material properties is covered from those for model fluids, to model dough, to actual dough, respectively. In this study there is no major difference found between model fluids and model dough so for Re = 0.8 not discussed for model dough, maximum attention has been given on model fluids and actual dough in this paper but results are given for model dough i.e., Re = 0.8 in tables.

4.1. **Effects of increasing inertia on velocity gradient, shear-rate, shear stress and power consumption for stationary stirrers:** For Re = 0.08 and Re = 8 computations are carried out to demonstrate the effect of increasing inertia upon velocity gradient, shear-rate, shear stress and power consumption. In figure−2, contour plots for stationary stirrers are presented. At a low level of inertia, Re = 0.08, contours of all variables demonstrate symmetric formations in the central region of the vessel, parallel to the stirrers and symmetrically intersecting the diameter that passes through the centres of the vessel and stirrers. Flow remains unaffected as Reynolds number rises to values of O(1), i.e., Re = 0.8; hence this data has been suppressed. However, upon increasing Reynolds number up to eight, so O(10), i.e., Re = 8.0; inertia takes hold and the contour region twist in the direction of rotation of the vessel and shifts towards the upper and lower-half plane, symmetry breakups in velocity gradient, shear-rate and shear stress and the material is pushed towards the vessel wall. The flow becomes asymmetric as a consequence of the shift in core of material upwards. The trend of rise in maxima and drop in minima is observed and the values are tabulated in Table−1.

Similar symmetry arguments apply across the geometry variants in all variables, at Re = 0.08, symmetric isobars for velocity gradient, shear-rate, shear stress and power consumption appear with unequal magnitude in non-dimensional positive extrema and negative minima on the two sides (upper and lower) of the stirrers in the narrow-gap. As inertia increases from Re = 0.8 to Re = 8, asymmetric contours are observed in all variables and across all instances, with positive maximum on the top of the stirrers and negative minimum at the outer stirrers tip (near the narrow-gap), see also Table−1. In non-dimensional terms above Re = 0.08 (noting scale differences), there is increase in velocity gradient, shear-rate and shear stress rise by as much as two percent in positive maxima, at Re = 8.0. However, in-contrast, the first stress difference decrease in same order approximately is observed. Whilst in power consumption and work-done which is about ten percent increase in maxima is observed with increasing inertia. The graph of work-done and power consumption is plotted in figure−3 against non-dimensional time step variants. Initially, work-done and power consumption is very high to drive the flow in the vessel. Subsequently, this high value for power consumption decreases gradually and reaches at some plateau for steady-state solution. Whilst, sum of work-done increase in same fashion up to steady-state.

4.2. **Effects of increasing inertia on velocity gradient, shear-rate, shear stress and power consumption for co-rotating stirrers:** Contours of all variables velocity gradient, shear-rate, shear stress and power consumption with increasing Reynolds number 0.08 to

TABLE 1. Various variables for stationary stirrers with Newtonian fluids (μ_0 = 105, 10.5 and 1.05 Pas);

Variables	Re = 0.08		Re = 0.8		Re = 8.0	
	Minima	Maxima	Minima	Maxima	Minima	Maxima
Velocity gradient	-1.14461	-1.14461	-1.14293	4.46645	-1.15125	4.68969
Shear rate	0.00	4.4631	0.002	4.46645	0.00	4.68969
Shear stress	-1.03394	2.23155	-1.05805	2.23322	-1.33561	2.41851
Stress Difference	-6.03566	6.0248	-6.08941	5.98074	-6.90787	5.79796
Power	0	19.9192	0	19.9491	0	21.9932

8.0 and increasing rotational speed of the stirrers for half, same and double presents in figure -4, -6 and -8 respectively, in the same direction of the rotation of the vessel for co-rotating stirrers.

As inertia increase from Re = 0.08 to Re = 8, asymmetric contours are observed, with positive maxima on the top of the both stirrers and negative minima at the outer stirrers tip, numerical results are shown in the Table-2. In the narrow gap, where stirrers rotates in the same direction of the vessel rotation, small values in minima and maxima appear for all variable instances and these values further decrease as the speed of stirrers decrease at low value of Re = 0.08. The increase in minima and maxima is observed and strengthen approximately from double to four times with increase in inertia at Re = 8.0.

For all instances, comparable equilibrium influence apply across the geometry variants in minima and maxima of velocity gradient, shear-rate and shear-stress, at Re = 0.08 and double rotational speed of stirrers, symmetric contours appear with equal magnitude in non-dimensional positive and negative extrema on both sides (upper and lower) of both stirrers in the narrow-gap as shown in figure-8.

The associated values of all variables are tabulated in Table-2 with increasing the speed of stirrers against the speed of vessel from half to double. As speed of stirrers increase, increase in the minima and maxima are noted for all cases at both inertial values. The velocity gradients are somewhat symmetrical in geometry at maxima and minima at twice the speed of stirrers and at half the speed of stirrers for both inertial values Re = 0.08 and Re = 0.8. However, upon increasing Reynolds number up to eight, thus O(10), inertia takes hold the tabulated variables are observed asymmetrical and the maxima and minima are also increase. Increasing the speed of the stirrers to double increases the power consumption remains same in minima and in contrast it increase up to twenty five percent in positive maxima.

In figure-5, -7 and -9 , the graph of work-done and power consumption is shown against non-dimensional time step variants. Initially, work-done and power consumption is very high to drive the flow in the vessel. Subsequently, this high value for power consumption decreases fastely at a stage and reaches at some plateau for steady-state solution for co-rotating stirrers at the half and same speed but for double speed this passion is changed and decreases gradually. Whilst, work-done increase in same fashion up to steady-state.

TABLE 2. Various variables for co-rotating stirrers with Newtonian fluids (μ_0 = 105, 10.5 and 1.05 Pas);

Variables	Speed	Re = 0.08		Re = 0.8		Re = 8.0	
		Minima	Maxima	Minima	Maxima	Minima	Maxima
Velocity gradient	Half	-0.11208	2.00842	-0.13028	2.01165	-0.28207	2.18178
	Same	-0.45398	1.69145	-0.45478	1.68572	-0.53672	1.9848
	Double	-5.37553	4.54706	-5.41958	4.57853	-7.24099	6.49085
Shear rate	Half	0.00083	1.87109	1.87432	1.87432	0.00173	4.34502
	Same	0.00051	1.30313	1.29741	1.29741	0.00142	9.89532
	Double	0.02125	5.92486	5.96891	5.96891	0.00394	33.1876
Shear stress	Half	-0.39279	1.00421	-0.4102	1.00583	-0.5839	1.79271
	Same	-0.44277	0.84572	-0.5126	0.84286	-1.1181	0.94252
	Double	-2.68777	2.27353	-3.1924	2.28926	-7.473	4.65567
Stress difference	Half	-2.69669	2.6867	-2.74653	2.64657	-3.5136	2.44376
	Same	-2.12539	2.45995	-1.96852	2.3089	-1.3368	3.62055
	Double	-7.31813	7.38789	-7.07431	7.85733	-5.74278	16.7961
Power	Half	0	3.50097	0	3.51308	0	4.17976
	Same	0	1.69814	0	1.70324	0	2.24019
	Double	0	35.104	0	35.6279	0	35.6742

4.3. **Effects of increasing inertia on velocity gradient, shear-rate, shear stress and power consumption for contra-rotating stirrers:** Increasing Reynolds number from Re = 0.08 to Re = 8.0 for contra-rotating double stirrers, equivalent field kinematic data in all variables is presented in figure−10 for half speed, figure−12 for same speed and figure−14 for double speed of the stirrers against the speed of the vessel, to make direct comparisons across all occurrences for Newtonian fluids, with particular reference to localised velocity gradient, shear-rate, shear stress and power consumption.

Isobars are shown for increasing speed of the stirrers from half speed to double speed display symmetry patterns at low inertial value Re = 0.08 and asymmetric configuration at higher value of inertia Re = 8.0 is shaped. In compare to the stationary stirrer case where formation of Newtonian stresses and other parameters are symmetric for all instances and at the same parameters asymmetric formation is observed, see figures−10, −12 and −14. At Re = 0.08, when increases the speed of stirrers for half, same and double respectively, no symmetry break-up is observed but at Re = 8, introducing the motion of stirrers from half speed to double speed of the stirrers effective changes has been observed in the stresses and other variables.

The graph illustrates the work-done over time interval and power consumption at all comparable parameter values for contra-rotating instances in figure−11, 13 and 15 for half speed, same speed and double speed of stirrers respectively. The behaviour for all instances is same, however, for both Reynolds numbers the comparable values are much higher and is almost ten times from half speed to double speed of the stirrers.

The tabulated values are in Table−3, minima and maxima for various variables. For velocity gradient, shear-rate, shear-stress and first stress difference between azimuthal and radial stresses, increase in the speed of stirrers from half to double, increase in the minima is observed. At low inertial value, Re = 0.08, this increase is almost double, however, at higher value of inertial, Re = 8, is approximately double to four times increase is noted. Whilst for power consumption is about five times approximately.

TABLE 3. Various variables for contra−rotating stirrers with Newtonian fluids (μ_0 = 105, 10.5 and 1.05 Pas);

Variable	Speed	Re=0.08		Re=0.8		Re=8.0	
		Minima	Maxima	Minima	Maxima	Minima	Maxima
Velocity gradient	Half	-2.58992	6.92803	-2.58798	6.92932	-2.43719	7.02753
	Same	-4.01149	9.38669	-4.01449	9.38694	-5.59621	9.5513
	Double	-6.8582	14.306	-6.90486	14.3229	-11.4476	16.8857
Shear rate	Half	0.00089	7.06537	0.00218	7.06665	0.00806	7.16486
	Same	0.00514	9.66136	0.00502	9.66161	0.00408	6.82598
	Double	0.01690	14.8553	0.011238	14.8423	0.00481	22.4677
Shear stress	Half	-1.67833	3.46402	-1.68435	3.46468	-1.74401	3.51377
	Same	-2.3286	4.69335	-2.40102	4.69347	-3.21727	8.90697
	Double	-3.64196	7.153	-3.96812	7.16147	-8.93301	20.743
Stress difference	Half	-9.38309	9.38414	-9.38008	9.39063	-9.46162	9.56863
	Same	-2.7151	12.741	-12.6002	2.8584	-11.7256	15.1497
	Double	-19.3628	19.4766	-8.8845	20.0245	-16.9897	36.4228
Power	Half	0	49.9194	0	49.9376	0	51.3353
	Same	0	93.3419	0	93.3466	0	96.5495
	Double	0	220.681	0	221.184	0	289.588

4.4. **Effects of increasing inertia on velocity gradient, shear−rate, shear stress and power consumption for mix−rotating stirrers:** For mix-rotating stirrers, the field kinematics data with increasing Reynolds number from 0.08 to 8.0 with particular reference to localised velocity gradient, shear-rate, shear stress and power consumption are shown in figure −16, −18 and −20 for half, same and double speed of stirrers respectively to make direct comparisons across all instances for Newtonian fluids. For this case, interested phenomena arise. In the case of half speed at low inertial value Re = 0.08, isobars are noted in around of the stirrer rotate in same direction of vessel and in right and left of the stirrer rotate in opposite direction of vessel with symmetric pattern in upper and lower region of vessel. When inertia increase upto Re = 8.0 isobars twist towards the upper region in the direction of rotation of the vessel. Whenever, situation examines vice-versa in the case of same speed of the stirrers.

Isobars are shown for double speed of the stirrers demonstrates symmetry patterns at low value of Reynolds number Re = 0.08 is formed in upper and lower region of the vessel.

TABLE 4. Various variables for mix-rotating stirrers with Newtonian fluids (μ_0 = 105, 10.5 and 1.05 Pas);

Variable	Speed	Re=0.08		Re=0.8		Re=8.0	
		Minima	Maxima	Minima	Maxima	Minima	Maxima
Velocity gradient	Half	-0.11208	2.00842	-0.13028	2.01165	-0.28207	2.18178
	Same	-0.45398	1.69145	-0.45478	1.68572	-0.53672	1.9848
	Double	-5.37553	4.54706	-5.41958	4.57853	-7.24099	6.49085
Shear rate	Half	0.004395	4.70657	0.004183	7.41495	0.00363	8.02225
	Same	0.003052	10.3516	0.002647	10.368	0.00142	11.6491
	Double	0.026373	16.2418	0.026461	14.2848	0.02993	21.8123
Shear stress	Half	-2.04905	3.63462	-2.04643	3.63881	-2.11429	3.94246
	Same	-4.05551	5.03848	-4.05503	5.04669	-5.24735	5.68721
	Double	-8.46209	8.15661	-8.48911	8.19283	-21.4674	10.9102
Stress difference	Half	-9.87923	9.8799	-9.88829	9.89485	-10.742	10.7666
	Same	-3.6366	13.6632	-13.5415	13.807	-14.1731	18.239
	Double	-2.3713	21.4936	-20.8918	22.1177	-20.7601	45.2794
Power	Half	0	54.8573	0	54.9815	0	64.3564
	Same	0	107.156	0	107.496	0	135.701
	Double	0	263.796	0	265.196	0	405.861

In contrast to the half and same speed of mix-rotating stirrers case where formation of Newtonian stresses and other parameters are symmetric for all instances, see figures − 20. At Re = 0.08 and for double speed of stirrers, no symmetry break-up is observed. However, at Re = 8, effective has been observed in the stresses and other variables and isobars twist towards the upper and lower region in the rotational direction of the vessel.

In figure −17, −19 and 21, for mix-rotating instances, graphs illustrate the work-done over time interval and power consumption at all comparable parameter values. The behaviour for all instances is same, however, for both Reynolds numbers the comparable values are much higher and is almost ten times from half speed to double speed of the stirrers.

Minima and maxima for velocity gradient, shear-rate, shear-stress, first stress difference and power consumption are tabulated in the Table4, increase in the speed of stirrers from half to double, increase in the minima is observed. At low inertial value, Re = 0.08, this increase is almost double, however, at higher value of inertial, Re = 8, is approximately three times. Whilst for is about eight times.

5. CONCLUSIONS

The use of a numerical flow simulator as a prediction tool for this industrial flow problem has been successfully demonstrated. For this complex mixing process, using Newtonian fluid, physically realistic simulations have been provided.

Addressing the rotation of the double stirrer case with stationary stirrers against the three cases of rotating stirrers in co-rotating, contra-rotating and mix-rotating directions are investigated with increasing inertia form Re = 0.08 to Re= 8.0. For stationary stirrers case, it is clearly demonstrated contours of all variables demonstrate symmetric formations in the central region of the vessel, parallel to the stirrers at Re = 0.08 and asymmetric when inertia reaches at Re = 8.0 and material moves in the direction vessel rotation.

The associated values of all variables for the case of co-rotating stirrers as speed of stirrers increase, increase in the minima and maxima are noted for all cases at both inertial values. The velocity gradients are somewhat symmetrical in geometry at maxima and minima at twice the speed of stirrers and at half the speed of stirrers for both inertial values variables are observed asymmetrical and the maxima and minima are also increase. Increasing the speed of the stirrers to double increases the power consumption remains same in minima.

In the case of contra-rotating Isobars are shown for half speed to double speed display symmetry patterns at low inertial value and asymmetric configuration at higher value of inertia. When increases the speed of stirrers from half to double, no symmetry break-up is observed but at higher inertia, introducing the motion of stirrers from half speed to double speed of the stirrers effective changes has been observed in the stresses and other variables.

Minima and maxima for velocity gradient, shear-rate, shear-stress, first stress difference and power consumption in the case of mix-rotating stirrers, increase in the speed of stirrers from half to double, increase in the minima is observed. At low inertial value, Re = 0.08, this increase is almost double, however, at higher value of inertial, Re = 8, is approximately three times.

Through the predictive capability generated, we shall be able to relate this to mixer design that will ultimately impact upon the processing of dough products. Promising future directions of this work are investigation of rotation of two stirrers case in co-rotating, contra-rotating and mix-rotating directions, changing material properties using non-Newtonian fluids and further introducing agitator in concentric configured stirrers in future.

Acknowledgement

The authors are greatly acknowledged to the Mehran University of Engineering and Technology, Jamshoro, for providing computational facility and financial grant of Higher Education Commission of Pakistan.

REFERENCES

[1] K. S. Sujatha, M. F.Webster, D. M. Binding, M. A. Couch, *Modelling and experimental studies of rotating flows in part-filled vessels: wetting and peeling, J. Foods Eng.*, **57**, (2002), 67−79.

[2] D. M. Binding, M. A. Couch, K. S. Sujatha, M. F. Webster, *Experimental and numerical simulation of dough kneading in filled geometries, J. Foods Eng.***57**, (2002) 1−13.

[3] K. S. Sujatha,, D. Ding, M. F. Webster, *Modelling three-dimensions mixing flows in cylindrical-shaped vessels, in: ECCOMAS CFD - 2001, Swansea, UK*, (2001) 1−10.

[4] K. S. Sujatha,, D. Ding, M. F. Webster, *Modelling of free surface in two and three dimensions, in: C. A. Brebbia, B. Sarlen (Eds.), Sixth International Conference on Computational Modelling of Free and Moving Boundary Problems - 2001, WIT, Lemnos, Greece*, (2001) 102−111.

[5] D. Ding, M. F. Webster, *Three-dimensional numerical simulation of dough kneading, in: D. Binding, N. Hudson, J. Mewis, J.-M. Piau, C. Petrie, P. Townsend, M. Wagner, K. Walters (Eds.), XIII Int. Cong. on Rheol., Vol. 2, British Society of Rheology, Cambridge, UK*, (2000) 318−320.

[6] N. Phan-Thien, M. Newberry and R. I. Tanner, *Non-linear oscillatory flow of a solid-like viscoelastic material, J. Non-Newtonian Fluid Mech.*, **92**, (2000) 67−80.

[7] P. M. Portillo, F. J. Muzzio and M. G. Ierapetritou, *Hybrid DEM-Compartment Modelling Approach for Granular Mixing, AIChE Journal*, **53(1)**, (2007) 119−128.

[8] A. Baloch, P. W. Grant and M. F. Webster, M. F., *Parallel Computation of Two-Dimensional Rotational Flows of the Viscoelastic Fluids in Cylindrical Vessel, Int. J. Comp. Aided Eng. and Software, Eng. Comput.*, **19(7)**, (2002) 820−853.

[9] A. Baloch, G. Q. Memon, and M. A. Solangi, *Simulation of Rotational Flows in Cylindrical Vessel with Rotating Single Stirrer, Punjab University Journal of Mathematics*, **40**, (2008) 83−96.

[10] A. Baloch, and M. F. Webster, M. F., *Distributed Parallel Computation for Complex Rotating Flows of Non-Newtonian Fluids, Int. J. Numer. Meth. Fluids*, **43**, (2003) 1301−1328.

[11] P. Townsend and M. F. Webster, *An algorithm for the three-dimensional transient simulation of non-Newtonian fluid flows, in: G. Pande, J. Middleton (Eds.), Proc. Int. Conf. Num. Meth. Eng.: Theory and Applications, NUMETA, Nijhoff, Dordrecht*, **T12** (1987) 1−11.

[12] D. M. Hawken, H. R. Tamaddon-Jahromi, P. Townsend, M. F. Webster, *A Taylor-Galerkin-based algorithm for viscous incompressible flow, Int. J. Num. Meth. Fluids*, **10**, (1990) 327−351.

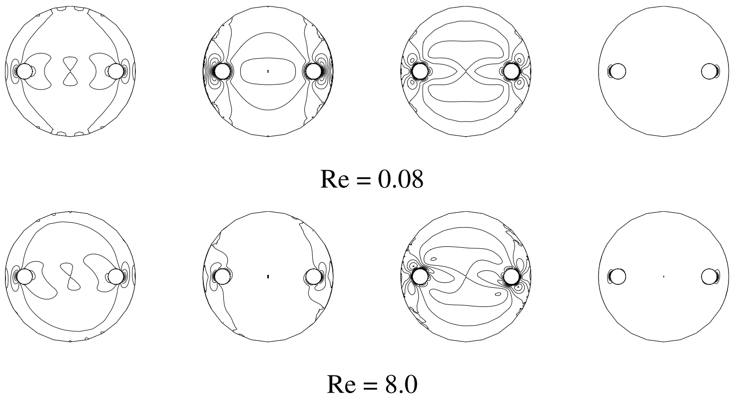

FIGURE 2. Contour plots of Velocity gradient, Shear-rate, Shear stress and Power for stationary stirrers for Newtonian fluid with increasing Reynolds number.

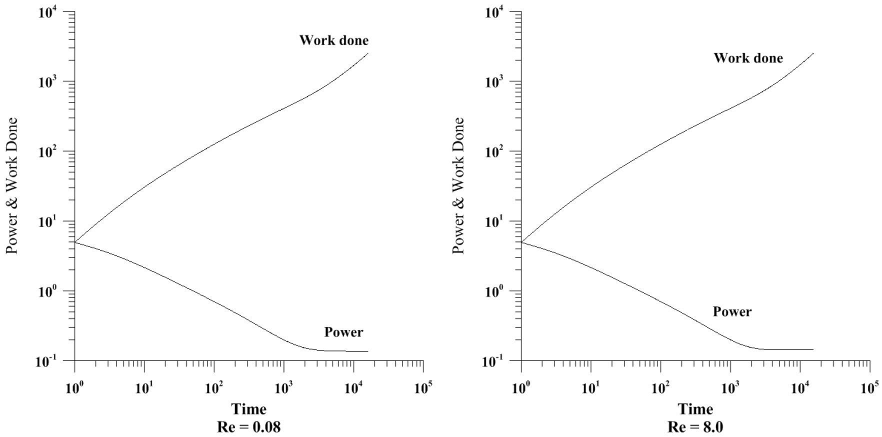

FIGURE 3. Graphs of power and work done for stationary stirrers for Newtonian fluid with increasing Reynolds number.

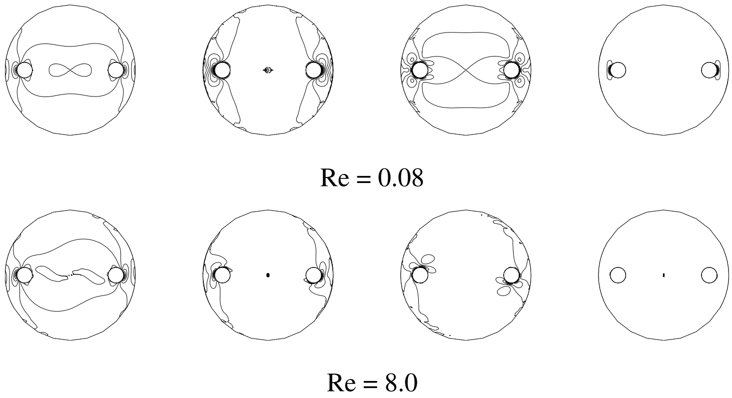

FIGURE 4. Contour plots of Velocity gradient, Shear-rate, Shear stress and Power for co-rotating stirrers with half speed for Newtonian fluid with increasing Reynolds number.

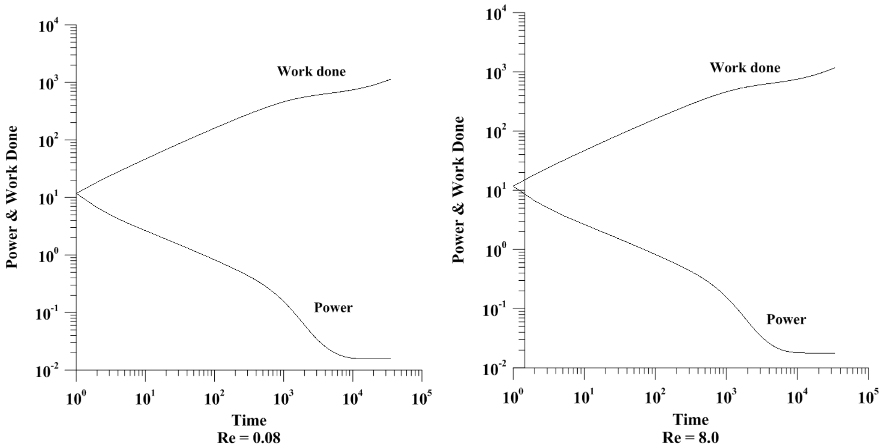

FIGURE 5. Graphs of power and work done for co-rotating stirrers with half speed for Newtonian fluid with increasing Reynolds number.

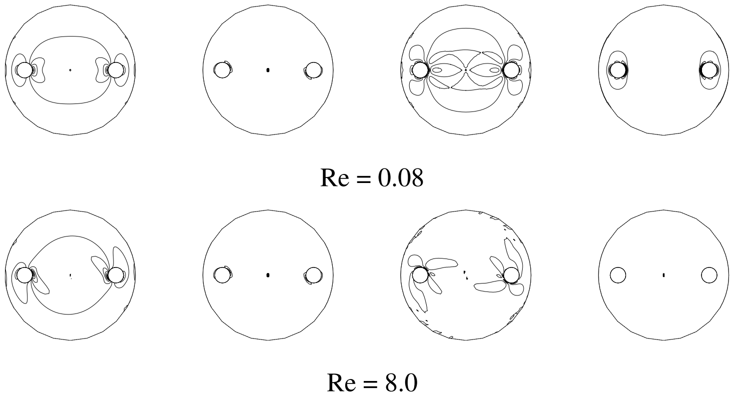

FIGURE 6. Contour plots of Velocity gradient, Shear-rate, Shear stress and Power for co-rotating stirrers with same speed for Newtonian fluid with increasing Reynolds number.

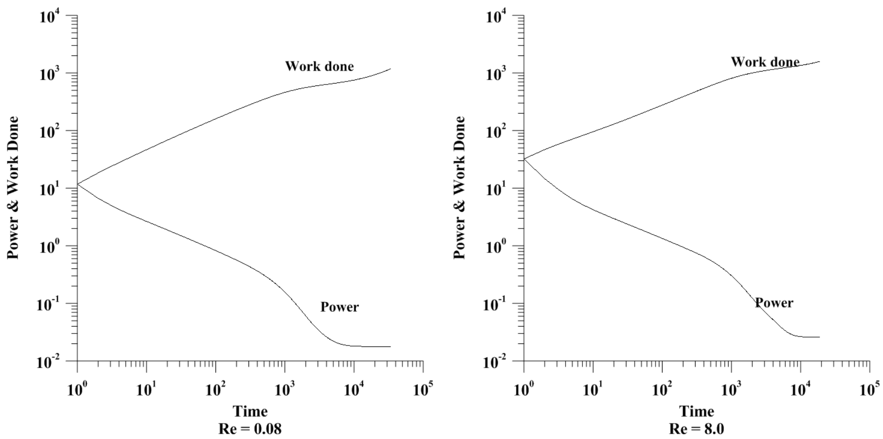

FIGURE 7. Graphs of power and work done for co-rotating stirrers with same speed for Newtonian fluid with increasing Reynolds number.

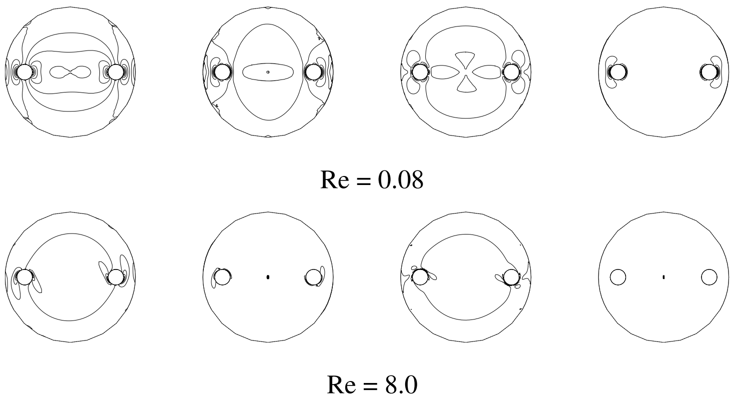

FIGURE 8. Contour plots of Velocity gradient, Shear-rate, Shear stress and Power for co-rotating stirrers with double speed for Newtonian fluid with increasing Reynolds number.

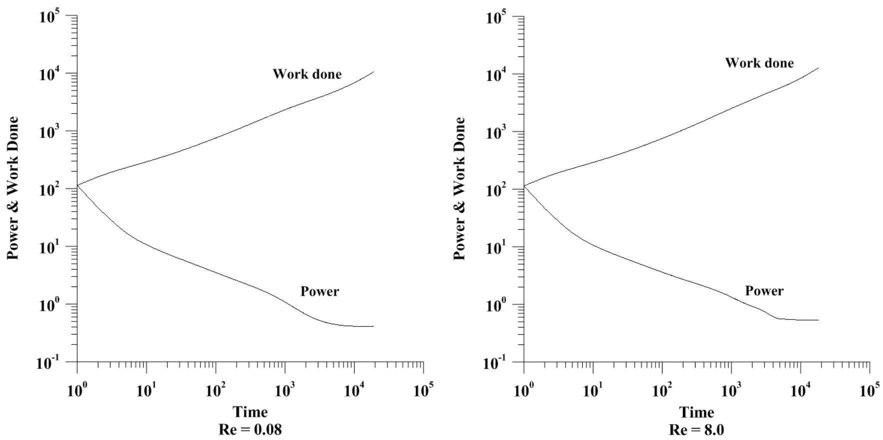

FIGURE 9. Graphs of power and work done for co-rotating stirrers with double speed for Newtonian fluid with increasing Reynolds number.

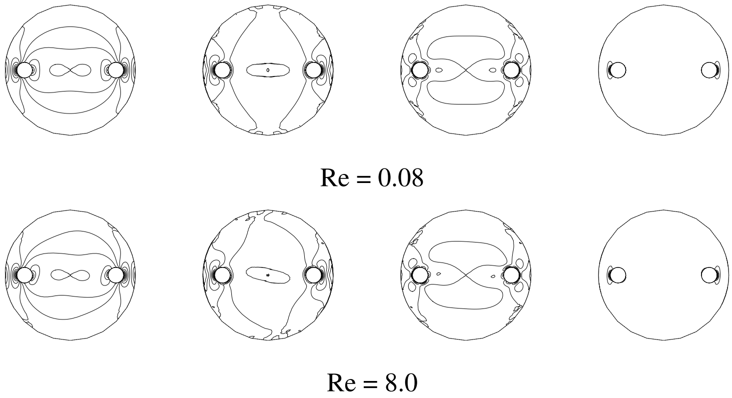

FIGURE 10. Contour plots of Velocity gradient, Shear-rate, Shear stress and Power for contra-rotating stirrers with half speed for Newtonian fluid with increasing Reynolds number.

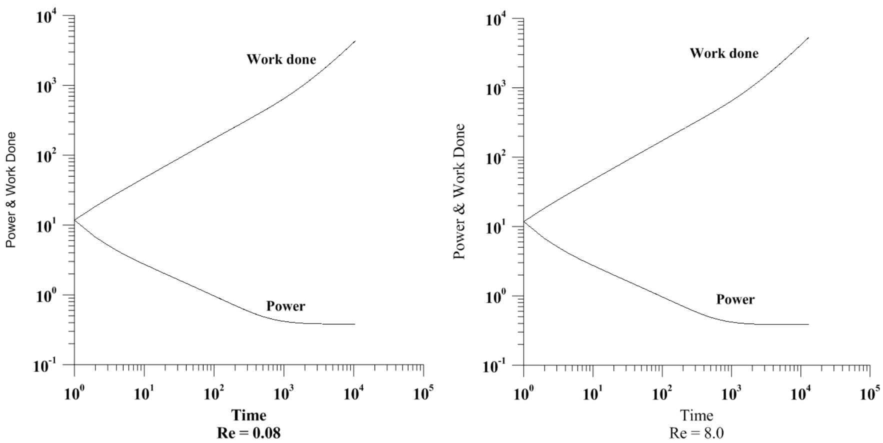

FIGURE 11. Graphs of power and work done for contra-rotating stirrers with half speed for Newtonian fluid with increasing Reynolds number.

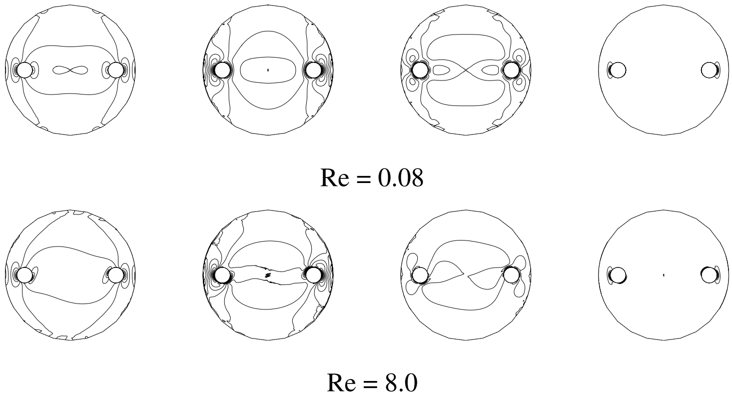

FIGURE 12. Contour plots of Velocity gradient, Shear-rate, Shear stress and Power for contra-rotating stirrers with same speed for Newtonian fluid with increasing Reynolds number.

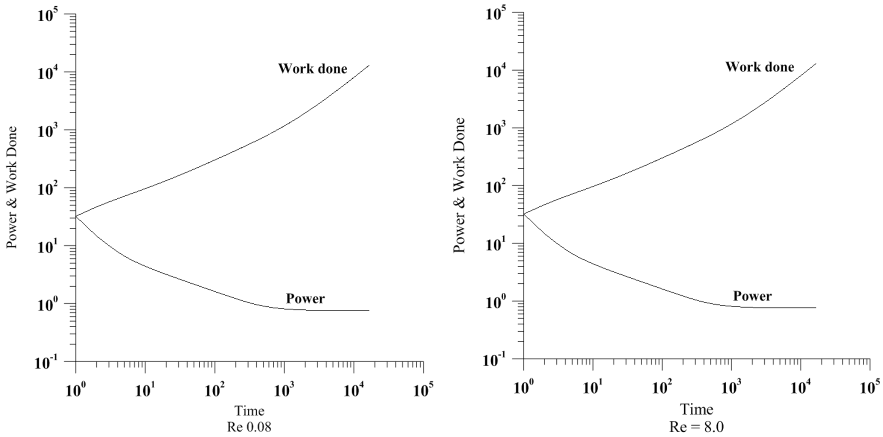

FIGURE 13. Graphs of power and work done for contra-rotating stirrers with same speed for Newtonian fluid with increasing Reynolds number.

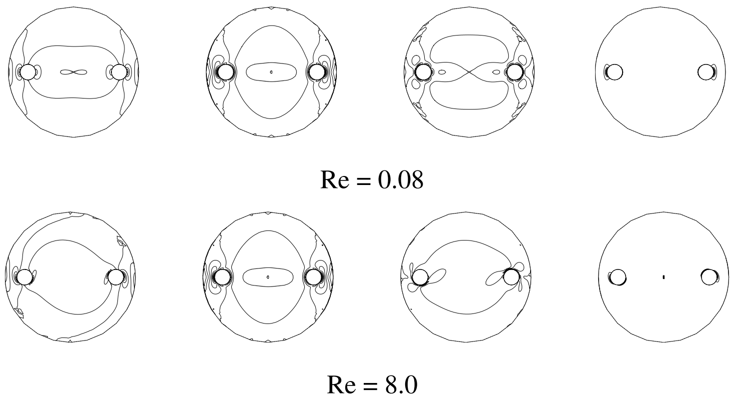

FIGURE 14. Contour plots of Velocity gradient, Shear-rate, Shear stress and Power for contra-rotating stirrers with double speed for Newtonian fluid with increasing Reynolds number.

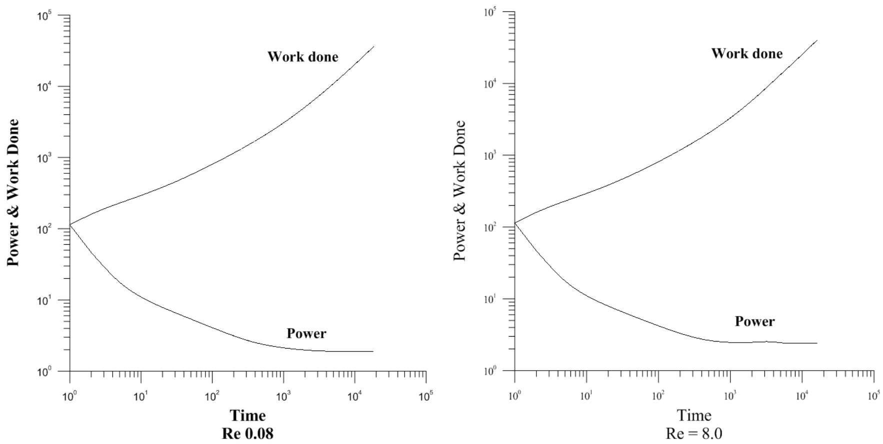

FIGURE 15. Graphs of power and work done for contra-rotating stirrers with double speed for Newtonian fluid with increasing Reynolds number.

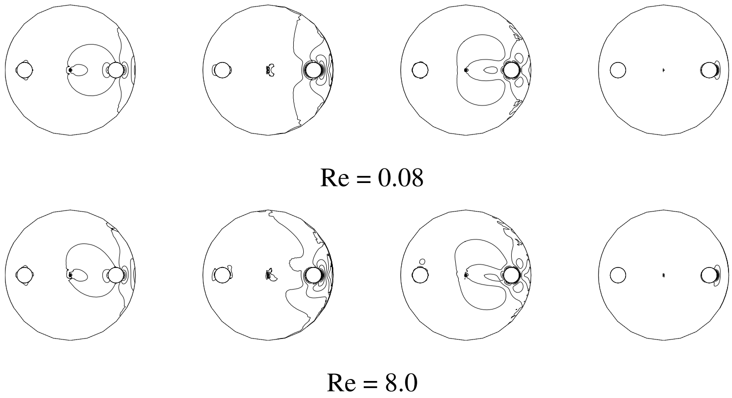

FIGURE 16. Contour plots of Velocity gradient, Shear-rate, Shear stress and Power for mix-rotating stirrers with half speed for Newtonian fluid with increasing Reynolds number.

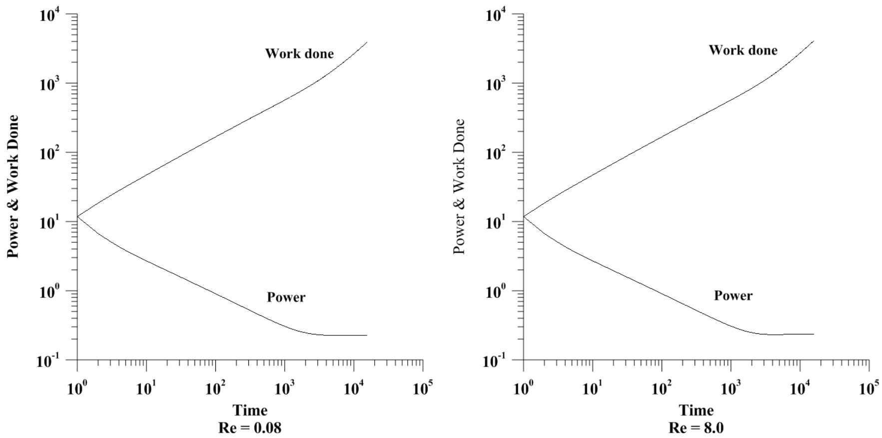

FIGURE 17. Graphs of power and work done for mix-rotating stirrers with half speed for Newtonian fluid with increasing Reynolds number.

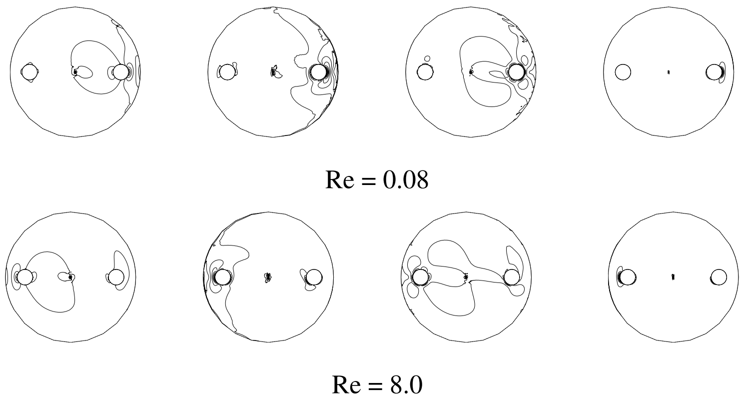

FIGURE 18. Contour plots of Velocity gradient, Shear-rate, Shear stress and Power for mix-rotating stirrers with same speed for Newtonian fluid with increasing Reynolds number.

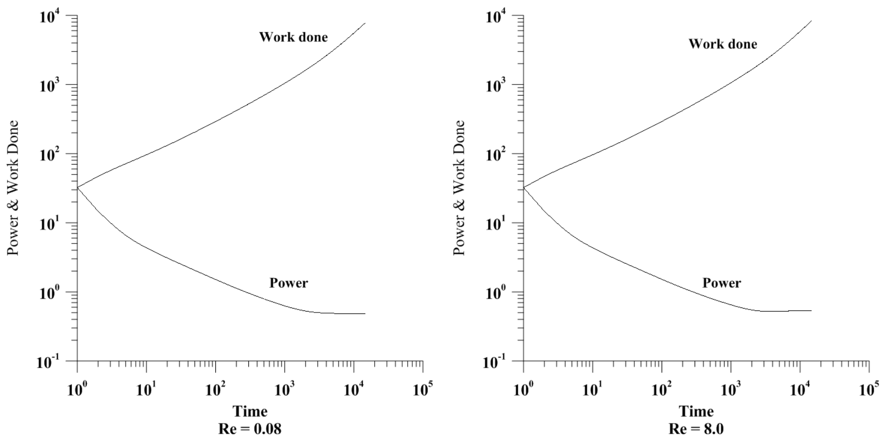

FIGURE 19. Graphs of power and work done for mix-rotating stirrers with same speed for Newtonian fluid with increasing Reynolds number.

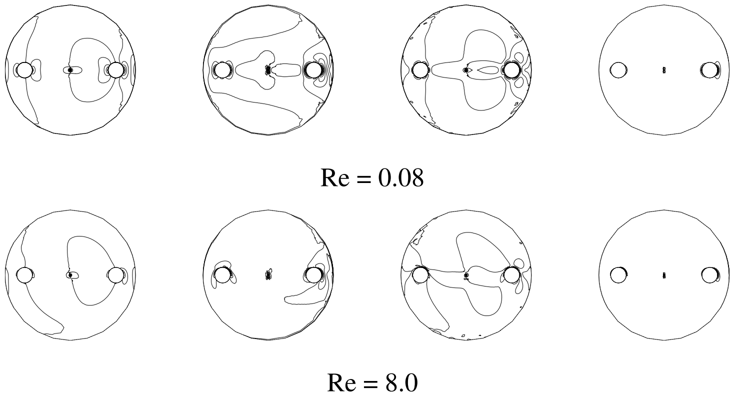

FIGURE 20. Contour plots of Velocity gradient, Shear-rate, Shear stress and Power for mix-rotating stirrers with double speed for Newtonian fluid with increasing Reynolds number.

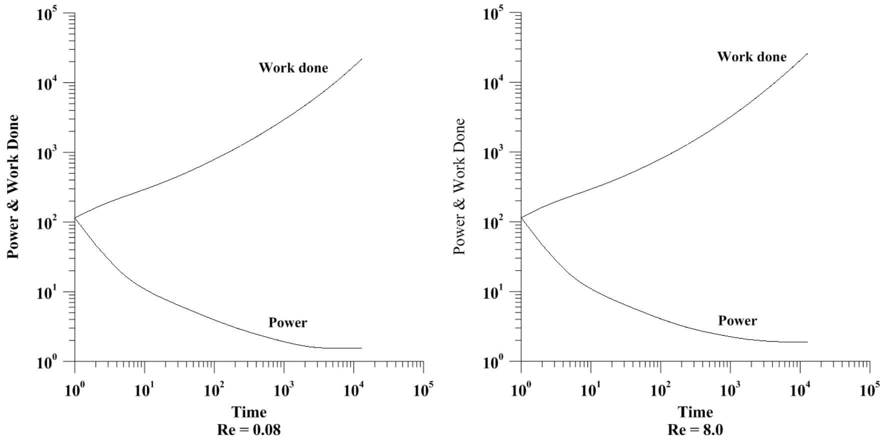

FIGURE 21. Graphs of power and work done for mix-rotating stirrers with double speed for Newtonian fluid with increasing Reynolds number.